

---

# ANALYTIC SELF-SIMILAR SOLUTIONS OF THE KARDAR-PARISI-ZHANG INTERFACE GROWING EQUATION WITH VARIOUS NOISE TERMS

---

A PREPRINT

**Imre Ferenc Barna**

Wigner Research Center  
Hungarian Academy of Sciences  
H-1525 Budapest, P.O. Box 49, Hungary  
barna.imre@wigner.mta.hu

**Gabriella Bognár**

Institute of Machine and Product Design  
University of Miskolc  
Miskolc-Egyetemváros 3515, Hungary

**Mohammed Guedda**

Faculte de Mathematiques et d'Informatique  
Université de Picardie Jules Verne Amiens  
33, rue Saint-Leu 80039 Amiens, France

**Krisztián Hriczó**

Institute of Mathematics  
University of Miskolc  
Miskolc-Egyetemváros 3515, Hungary

**László Mátyás**

Department of Technical and Natural Sciences  
Sapientia University  
Libertății sq. 1, 530104 Miercurea Ciuc, Romania

January 10, 2022

## ABSTRACT

The one-dimensional Kardar-Parisi-Zhang dynamic interface growth equation with the self-similar Ansatz is analyzed. As a new feature additional analytic terms are added. From the mathematical point of view, these can be considered as various noise distribution functions. Six different cases were investigated among others Gaussian, Lorentzian, white or even pink noise. Analytic solutions were evaluated and analyzed for all cases. All results are expressible with various special functions like Kummer, Heun, Whittaker or error functions showing a very rich mathematical structure with some common general characteristics.

**Keywords** self-similar solution · KPZ equation · Gaussian noise · Lorentzian noise · Special functions · Heun functions

## 1 Introduction

Growth patterns in clusters and sodification fronts are challenging problems from a long time. Basic knowledge of the roughness of growing crystalline facets has obvious technical applications [1]. The simplest nonlinear generalization of the ubiquitous diffusion equation is the so called Kardar-Parisi-Zhang (KPZ) model obtained from Langevin equation

$$\frac{\partial u}{\partial t} = \nu \nabla^2 u + \frac{\lambda}{2} (\nabla u)^2 + \eta(\mathbf{x}, t), \quad (1)$$

where  $u$  stands for the profile of the local growth [2]. The first term on the right hand side describes relaxation of the interface by a surface tension, which prefers a smooth surface. The second term is the lowest-order nonlinear term that can appear in the surface growth equation justified with the Eden model and originates from the tendency of the surface to locally grow normal to itself and has a non-equilibrium in origin. The last term is a Langevin noise to

mimic the stochastic nature of any growth process and has a Gaussian distribution usually. There are numerous studies available about the KPZ equation in the literature in the last two decades. Without completeness we mention some of them. The foundation of the physics of surface growth can be found in the book of Barabási and Stanley [3]. Hwa and Frey [4, 5] investigated the KPZ model with the help of the self-mode-coupling method and with renormalization group-theory, which is an exhaustive and sophisticated method using Green's functions. They considered various dynamical scaling form of  $C(x, t) = x^{-2\varphi} C(bx, b^z t)$  for the correlation function (where  $\varphi$ ,  $b$  and  $z$  are real constants). Lässig showed how the KPZ model can be derived and investigated with field theoretical approach [6]. In a topical review paper Kriecherbauer and Krug [7] derived the KPZ model from hydrodynamical conservation equations with a general current density relation. Later, Einax *et al.* [8] published a review study on cluster growth on surfaces.

Numerous models exist, which may lead to similar equations as the KPZ model, i.e., the interface growth of bacterial colonies [9]. More general interface growing models were developed based on the so-called Kuramoto- Sivashinsky (KS) equation which is similar to the KPZ model with and extra  $-\nabla^4 u$  term on the right hand side of (1) (see [10], [11]).

Guedda has already investigated the generalized deterministic KPZ equation, when the gradient term is on an arbitrary exponent, with the self-similar Ansatz [12]. Kersner and Vicsek investigated the traveling wave dynamics of the singular interface equation [13], which is closely related to the KPZ equation. Ódor and co-worker intensively examined the two dimensional KPZ equation with extended dynamical simulations to study the physical aging properties of different systems like glasses or polymers [14].

Beyond these continuous models based on partial differential equations (PDEs) there are numerous purely numerical methods available to study diverse surface growth phenomena. Without completeness, we mention the kinetic Monte Carlo [15], Lattice-Boltzmann simulations [16] and the etching model [17].

By present work, one may find certain kind of solutions to the problem [18, 19]. It is already mentioned in [20] these are for droplet initial conditions.

The first term on the right hand side of the equation can be also related to diffusion [21], and it can be found in the description of such processes [22, 23].

In this paper we analyze the solutions of the KPZ equation with the self-similar Ansatz in one-dimension applying various forms of the noise term. Numerical results are provided both for similarity solutions with similarity variables and for the solutions with the original variables as well. The effect of the parameters involved in the problem is examined.

The similarity method was used for the investigation of analytic solution of the two dimensional Navier-Stokes equation with a non-Newtonian type of viscosity [24].

## 2 Theory

Non-linear PDEs has no general mathematical theory, which could help us to derive physically relevant solutions. Basically, there are two different trial functions (or Ansatz) having well-founded physical interpretation. The first one is the traveling wave solution, which mimics the wave property of the investigated phenomena described by the non-linear PDE. The second one is the self-similar Ansatz of the form

$$u(x, t) = t^{-\alpha} f\left(\frac{x}{t^\beta}\right) := t^{-\alpha} f(\omega), \quad (2)$$

where  $u(x, t)$  can be an arbitrary variable of a PDE and  $t$  denotes time and  $x$  means spatial dependence. The similarity exponents  $\alpha$  and  $\beta$  are of primary physical importance since  $\alpha$  represents the rate of decay (or sharpening process if  $\alpha < 0$ ) of the magnitude  $u(x, t)$ , while  $\beta$  is the rate of spread (or contraction if  $\beta < 0$ ) of the space distribution for  $t > 0$ . The most powerful result of this Ansatz is the fundamental or Gaussian solution of the Fourier heat conduction equation (or for Fick's diffusion equation) with  $\alpha = \beta = 1/2$ . These solutions are exhibited on Fig. 1 for fixed times  $t_1 < t_2$ . We can generally state, that this Ansatz mimics the diffusive properties (the similarities to normal diffusion) of the investigated PDE. This is the key point why this Ansatz is used. We note, that in some cases [25] the traveling wave and self-similar solutions are intertwined and can be transformed into one another.

This transformation is based on the assumption that a self-similar solution exists, i.e., every physical parameter preserves its shape during the expansion. Self-similar solutions usually describe the asymptotic behavior of an unbounded or a far-field problem; the time  $t$  and the spacial coordinate  $x$  appear only in the combination of  $f(x/t^\beta)$ . It means that the existence of self-similar variables implies the lack of characteristic lengths and times. These solutions are usually not unique and do not take into account the initial stage of the physical expansion process. It is also transparent from (2) that to avoid singularity at  $t = 0$  the following transformation  $\tilde{t} = t + t_0$  is valid.

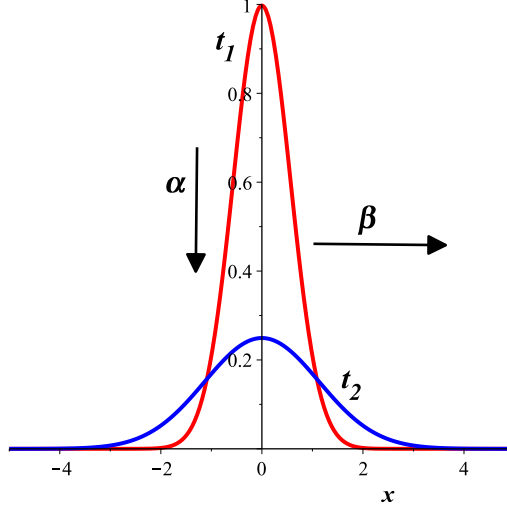


Figure 1: A self-similar solution of Eq. (2) for  $t_1 < t_2$ . The presented curves are Gaussians for regular heat conduction.

We should note that with the application of the Hopf-Cole transformation  $h = A \ln(y)$  the non-linear KPZ equation can be converted to the regular heat conduction (or diffusion equation) with a stochastic term.

There are numerous reasonable generalization of (2) available, one of them is  $u(x, t) = h(t) \cdot f[x/g(t)]$ , where  $h(t)$  and  $g(t)$  are continuous functions. The choice of  $h(t) = g(t) = \sqrt{t_0 - t}$  is a special kind, called the blow-up solution. It means that the solution becomes infinity after a well-defined finite time duration.

These kind of solutions describe the intermediate asymptotics of a problem. They hold when the precise initial conditions are no longer important, but before the system has reached its final steady state. For some systems it can be shown that the self-similar solution fulfills the source type (Dirac delta) initial condition. They are much simpler than the full solutions and so easier to understand and study in different regions of parameter space. A final reason for studying them is that they are solutions of a system of (ordinary differential equations (ODEs) and they do not suffer the extra inherent numerical problems related to PDEs. In some cases self-similar solutions helps us to understand global physical properties of the solutions like finite oscillations, diffusion-like properties, discontinuous solutions or the existence of compact supports. Such kind of general information is hard to find from purely numerical calculations.

Applicability of this Ansatz is quite wide and comes up in various mechanical systems [26], in transport phenomena like heat conduction [25], in Euler equation [27] or even in various two or three dimensional Navier-Stokes equations [28, 29].

### 3 Results without noise term

We start our investigation with the KPZ equation (1) in one spatial dimension neglecting the noise term ( $\eta(x, t) = 0$ ). Calculating the time and spacial derivatives of (2) and substituting to (1) one gets the following constrains for the exponents:  $\alpha = 0$  and  $\beta = 1/2$ . In regular heat conduction (or diffusion) process both exponents are equal to  $1/2$ , which means that the decay (perpendicular dynamics to the surface) and the spreading (parallel dynamics to the surface) of the solution have the same strength in time. For the KPZ equation the general features are different. Now,  $\alpha$  vanishes, which means that we cannot identify any kind of decaying dynamics of the solution perpendicular to the surface. The non-zero value of  $\beta$  can be understood as a kind of spreading parallel to the surface. These are general and relevant statements of the surface growth process described by our solution. The remaining non-linear ODE reads

$$\nu f''(\omega) + f'(\omega) \left[ \frac{\omega}{2} + \frac{\lambda}{2} f'(\omega) \right] = 0. \quad (3)$$

The general solution can be given with the logarithm of the error function

$$f(\omega) = 2 \frac{\nu}{\lambda} \ln \left( \frac{\lambda c_1 \sqrt{\pi \nu} \operatorname{erf}[\omega/(2\sqrt{\nu})] + c_2}{2\nu} \right), \quad (4)$$

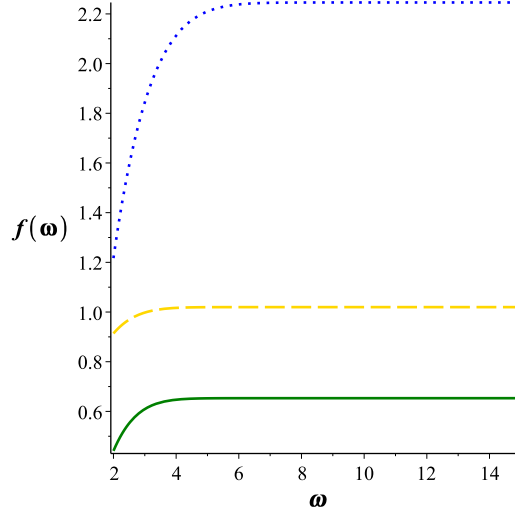


Figure 2: The self-similar solution of the KPZ equation without any noise term for  $c_1 = c_2 = 1$ . Solid line is for  $\lambda = \nu = 1$ , dashed line is for  $\nu = 1$  and  $\lambda = 2$  and the dotted line represents  $\nu = 2$  and  $\lambda = 1$ .

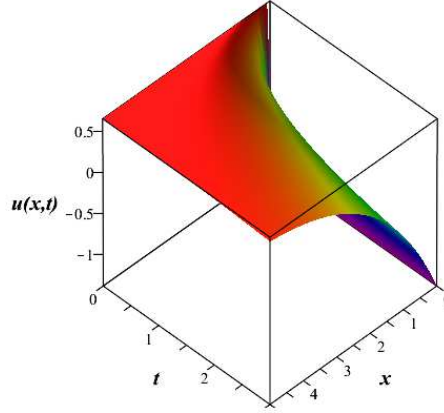


Figure 3: The self-similar solution of the original KPZ equation without the noise term for the parameter set  $c_1 = c_2 = \lambda = \nu = 1$ .

where  $erf$  is the error function [30] and  $c_1$  and  $c_2$  are integration constants. The role of  $c_2$  is just a shift of the solution. For physical reasons the surface tension  $\nu$  should be larger than zero. Analyzing the solution to Eq. (4), the value of  $\lambda$  should be positive as well. Figure 2 presents three different shape function solutions of the ODE with  $c_1 = c_2 = 1$  and for three different combinations of  $\lambda$  and  $\nu$ . Note, that all solution has the same simple qualitative behavior, a quick ramp-up and a converged plateau. Figure 3 shows the complete solutions of the original PDE showing the spatial and time dependence for  $c_1 = c_2 = \lambda = \nu = 1$ . The function has a similar structure like Fig. 2 a quick ramp-up and a slow convergent plateau. We may say that different numerical values of  $\eta$  and  $\nu$  do not drastically change the qualitative structure of the solution surface. A closer look of the solution shows, that at  $t = 0$  the height of the surface has a constant value, later at small times a thin valley is formed, which becomes wider and wider as time goes on. The physical parameters  $\lambda, \nu$  and the integration constants (only shifts the solutions) set the shape and the depth of the valley. Even at large times at large spatial distances, the height of the surface, i.e., the asymptotic solution remains constant. The growth of the valley (or void) can be understood as a kind of front propagation as well, and therefore can be explained with the non-zero  $\beta$  exponent.

At this point it comes clear to us, that any kind of surface growth mechanism can be only described and investigated with the additional noise term. The direct application of the self-similar solution to the KPZ equation without any additional noise term  $\eta(x, t)$  cannot describe any kind of growth process.

## 4 Results with various noise terms

It is obvious that every physical process is perturbed with some kind of perturbations. Perturbations which carry no information are called noise. The KPZ equation, very correctly, include an additive noise term. Our similarity Ansatz of the from (2) satisfy the general ODE with the form of

$$\nu f''(\omega) + f'(\omega) \left[ \frac{\omega}{2} + \frac{\lambda}{2} f'(\omega) \right] + t\eta(\omega) = 0. \quad (5)$$

If we want to apply the self-similar Ansatz (2) to the noisy KPZ equation than the noise term  $t\eta(x, t) = l(\omega) = l(x/t^\beta)$  should be some kind of analytic function of the original variables of  $x, t$ , on the other side, we want to handle noise in a statistically correct manner,  $\eta(x, t)$  should be a density function of a probability distribution as well. This second condition dictates that the density function should be positive and should have an existing finite integral on a finite or infinite support. Note, the extra time dependence of the last term in (5) is dictated from a dimensional analysis reason.

First, we investigate noises with various power-law dependencies  $l(\omega) = a\omega^n$ . Noises with different integer power values of  $n$  are named after different colors  $n = -2, -1, 0, 1$  which are brown, pink, white and blue, respectively. Two additional cases, the Gaussian and Lorentzian noises, are investigated as well. To avoid further misunderstanding we must state that in our calculations a Gaussian noise means that the noise term explicitly depends on the scaled spatial coordinate  $x/t^{1/2}$  and not on the Fourier spectra as usually considered. The argument  $\omega$  of the shape function is the time-scaled spatial coordinate and not the angular frequency. Of course, in principle it is possible to evaluate the Fourier spectra of our noise terms and interpret them in the frequency domain but that is not the aim of the present study.

### 4.1 Brown noise $n = -2$

Our first case leads to the ODE of

$$\nu f''(\omega) + f'(\omega) \left[ \frac{\omega}{2} + \frac{\lambda}{2} f'(\omega) \right] + \frac{a}{\omega^2} = 0. \quad (6)$$

Using the mathematical program package Maple 12, the solution can be obtained in a closed form

$$f(\omega) = -\frac{\omega^2}{4\lambda} + \frac{1}{\lambda} \left[ \ln((\omega^3 \lambda^2 \{c_1 M_{-\frac{1}{4}, \frac{d}{4}}(r) - c_2 W_{-\frac{1}{4}, \frac{d}{4}}(r)\}^2) / \right. \\ \left. (M_{\frac{3}{4}, \frac{d}{4}}(r) \cdot \nu \cdot W_{-\frac{1}{4}, \frac{d}{4}}(r) + M_{\frac{3}{4}, \frac{d}{4}}(r) \cdot \nu \cdot d \cdot W_{-\frac{1}{4}, \frac{d}{4}}(r) + \right. \\ \left. 4M_{-\frac{1}{4}, \frac{d}{4}}(r) \cdot \nu \cdot W_{\frac{3}{4}, \frac{d}{4}}(r))^2) \nu \right] 1, \quad (7)$$

where  $M$  and  $W$  are the Whittaker  $M$  and Whittaker  $W$  functions [30]. For the better transparency we used the following notations  $d = \sqrt{\nu^2 - 2\lambda a}/\nu$  for the second parameter and  $r = \omega^2/(4\nu)$  for the argument of the Whittaker functions. Both parameters of the Whittaker functions must be real numbers, which means that  $\nu^2 - 2\lambda a \geq 0$  therefore for any kind of fixed and positive  $\nu$  and  $\lambda$ , there is an upper limit for  $a$ , which is the strength of the noise term. So, if the magnitude of the noise reaches a definite level, the Whittaker function and the solution of the problem becomes undefined and meaningless. This is consistent with our physical picture about noisy processes.

Due to the Whittaker function, the solution is undefined for negative arguments  $\eta$  for any kind of parameter set. Figure 4 presents the solution of Eq. (7) for two different parameter sets. The numerical value of  $\nu$  defines the position of the singularity in a non trivial way, larger  $\nu$  shifts the position to larger arguments. At fixed physical parameters  $a, \nu$  and  $\lambda$ , the first integration constant  $c_1$  is equal with the asymptotic value of the solution for large arguments. The second integration constant  $c_2$  directly defines the function in the origin in a non-trivial way, the larger the value the larger the function as well.

Figure 5 shows the solution profile  $u(x, t)$  of the KPZ equation as the function of time and spatial coordinate. The sharp cusp is clearly seeing. It is also evident that the position of the cusp moves to larger spatial coordinates as time goes on, compared to the free KPZ solution of Eq. (3.1), which means that the additional noise term puts a small island into the origin which is growing and pushing the cusp before. Another interesting feature is that the cusps survives even at large times and is not filled up as would we expect from our physical intuition.

The sharp but finite cusp that arises in this solutions is the so-called Van Hove singularity, which was first seen in crystals in the function of elastic frequency distribution [31]. We note, that the finite number of peaks on Fig. 5 under the cusp are just an artifact of the finite resolution of the Maple software.

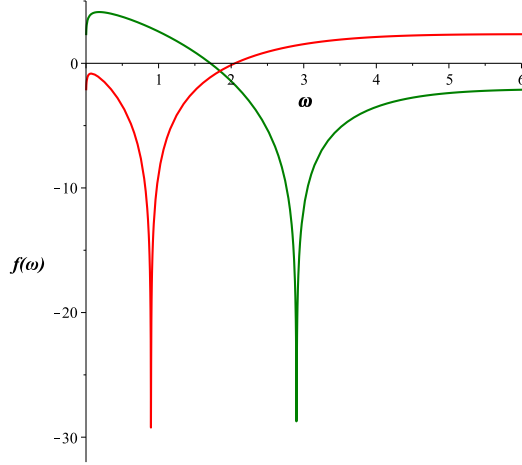


Figure 4: The shape functions of the Brownian noise Eq. (7) for  $a = \lambda = 1$ ,  $\nu = 2$  physical parameters. The red line is for  $c_1 = 3, c_2 = 1$  and the green line is for the integration constants  $c_1 = 1, c_2 = 3$ .

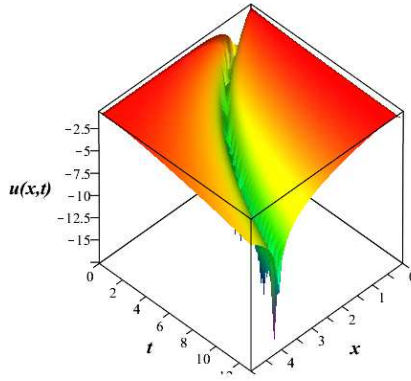


Figure 5: The solution of the KPZ eq. with Brownian noise, for the parameter set of  $\lambda = \nu = c_1 = c_2 = 1$  and  $a = 1/2$ .

#### 4.2 Pink noise $n = -1$

The corresponding ODE reads

$$\nu f''(\omega) + f'(\omega) \left[ \frac{\omega}{2} + \frac{\lambda}{2} f'(\omega) \right] + \frac{a}{\omega} = 0. \quad (8)$$

In the most general case when all three parameters are undefined ( $\lambda, \nu, a$ ), there is no closed formula available for the solution. There is an existing expression containing the integral of the HeunB functions [30] together with other functions. For given values ( $\lambda = \nu = a = 1$ ), the formula becomes a bit more transparent

$$f(\eta) = -\frac{1}{\eta^2} + 2 \ln \left[ \frac{c_1 \eta}{2} H_B \left( 1, 0, -1, 2, \frac{-\eta}{2} \right) - \frac{c_2 \eta}{2} H_B \left( 1, 0, -1, 2, \frac{-\eta}{2} \right) \times \left\{ \int \frac{e^{-\frac{\eta^2}{4}}}{\eta^2 H_B \left( 1, 0, -1, 2, \frac{-\eta}{2} \right)^2} \right\} \right]. \quad (9)$$

Unfortunately, if the strength of the noise  $a$  is different, then the term containing the integral of the function  $H_C$  cannot be separated from the pure  $H_C$  function and the final form cannot be evaluated numerically.

Figure 6 shows the shape function where the physical parameters are set to unity. At first sight, the solution looks the same as the solution without noise, however there is a small positive island, which is created next to the valley. In other words the solution has a local maximum at finite  $\omega$ , which means a finite time and space coordinate  $x/t^{\frac{1}{2}}$ . As

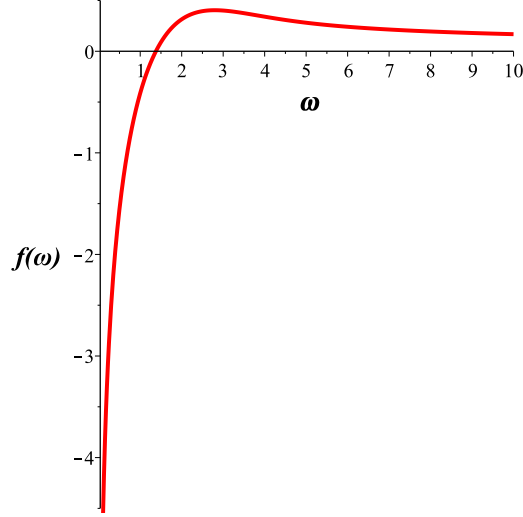


Figure 6: The shape function of the pink noise for  $a = \lambda = \nu = 1$  and for  $c_1 = 1$  and  $c_2 = 0$ .

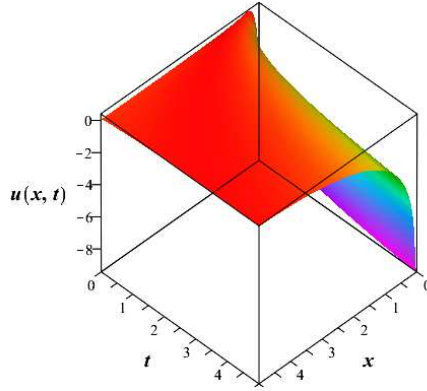


Figure 7: The complete solution of the KPZ equation for the pink noise with the parameters given above.

time goes on the valley becomes wider and wider pushing this tiny island to the right with a continuous smearing. We can say that the surface growing phenomena breaks down in the dynamics of this tiny island or rather "reef". So, there is no general surface growth phenomena along the whole axis.

Figure 7 shows the complete solution of the KPZ equation with the pink noise, note the tiny positive bump at small time and space coordinates.

### 4.3 White noise $n = 0$

The associated ODE is now

$$\nu f''(\omega) + f'(\omega) \left[ \frac{\omega}{2} + \frac{\lambda}{2} f'(\omega) \right] + c = 0. \quad (10)$$

There is no general closed formula available for a general real constant  $c$ . However, if the constant noise term is written in the form of  $\eta = n\lambda$ , which can be identified as a kind of external mechanism due to the work of [32], then other analytical solutions become available which can be expressed via Kummer  $M$  and Kummer  $U$  functions [30]

$$f(\omega) = \frac{2\nu}{\lambda} \ln \left( \left\{ \lambda \left[ -c_1 M \left( 1 - \frac{n\lambda}{2}, \frac{3}{2}, \frac{\omega^2}{n\lambda} \right) - c_2 U \left( 1 - \frac{n\lambda}{2}, \frac{3}{2}, \frac{\omega^2}{n\lambda} \right) \right] \right\} / \right. \\ \left. \left\{ \nu \left[ M \left( -\frac{n\lambda}{2}, \frac{3}{2}, \frac{\omega^2}{n\lambda} \right) U \left( 1 - \frac{n\lambda}{2}, \frac{3}{2}, \frac{\omega^2}{n\lambda} \right) + \right. \right. \right.$$

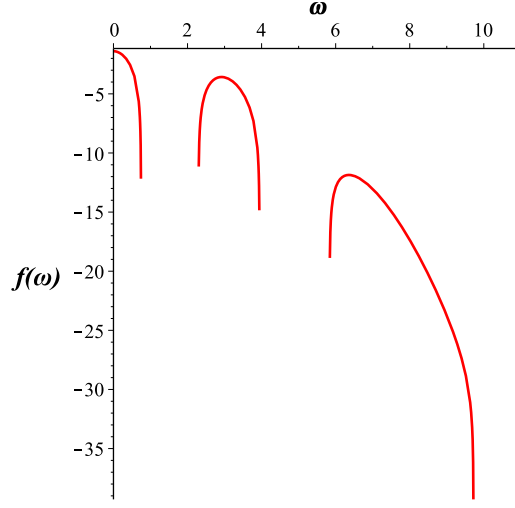


Figure 8: The shape function for the white noise for parameter set  $a = \lambda = \nu = 1 = c_1 = c_2 = 1$ .

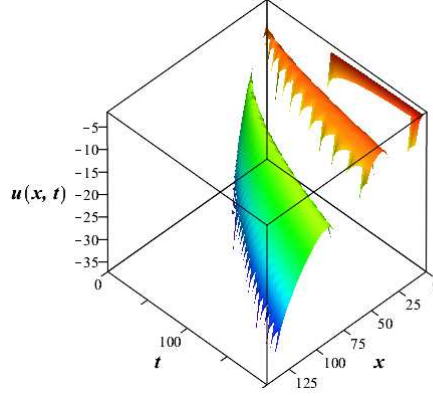


Figure 9: The complete solution for the white noise for  $a = 1/2, \lambda = 2, \nu = 1/2$  and for  $c_1 = c_2 = 1$ .

$$n\lambda M\left(-\frac{n\lambda}{2}, \frac{3}{2}, \frac{\omega^2}{n\lambda}\right) U\left(1 - \frac{n\lambda}{2}, \frac{3}{2}, \frac{\omega^2}{n\lambda}\right) + 2M\left(1 - \frac{n\lambda}{2}, \frac{3}{2}, \frac{\omega^2}{n\lambda}\right) U\left(-\frac{n\lambda}{2}, \frac{3}{2}, \frac{\omega^2}{n\lambda}\right) \Bigg] \Bigg\} - \frac{2\nu \ln(2)}{\lambda}. \quad (11)$$

Figure 8 shows the shape function for the white noise. The new feature is that the solution fell apart to numerous distinct intervals with compact supports. The function has large but finite negative values at the supports with infinitely large derivatives, which can be called cusps as well. Note, that there are finite intervals where the solution is not defined. Figure 9 shows the solution  $u(x, t)$  of the KPZ equation. We mention that the separate islands continuously grow as time goes on, but, they cannot touch each other even at large times. The finite number of peaks under the cusp are again an artifact of the finite resolution of the Maple software. Such kind of surface growth, where separate "barrys" are created, can be noticed on coral reefs or on dripstones.

#### 4.4 Blue noise $n = 1$

The last power law noise case is the following

$$\nu f''(\omega) + f'(\omega) \left[ \frac{\omega}{2} + \frac{\lambda}{2} f'(\omega) \right] + a\omega = 0. \quad (12)$$



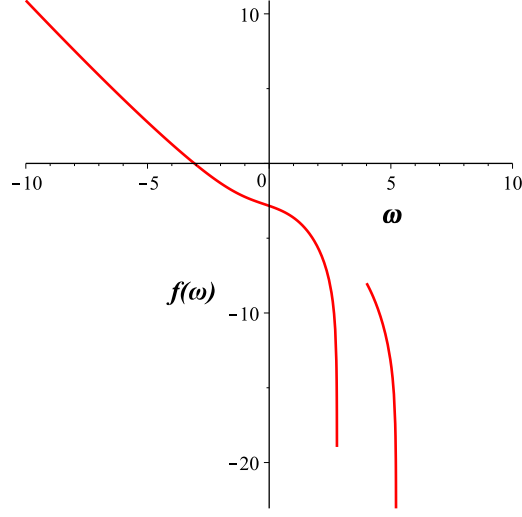


Figure 10: The shape function of the blue noise for the parameter set  $a = \lambda = \nu = 1$  and initial conditions  $c_1 = 1$  and  $c_2 = 1$ , respectively.

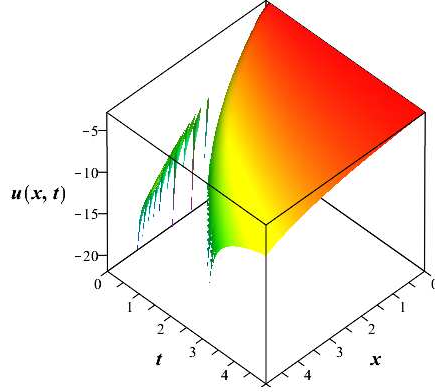


Figure 11: The complete solution  $u(x, t)$  for the blue noise with the parameters given above.

The structure of the solution shows some similarity to the brown and white noise and can be expressed with the help of the Kummer  $U$  and  $M$  functions

$$f(\omega) = -2\omega + 2\frac{\nu}{\lambda} \ln \left\{ \frac{-\lambda(4\lambda - \omega) [c_2 U(\epsilon_-, \frac{1}{2}, \sigma) - c_1 M(\epsilon_-, \frac{1}{2}, \sigma)]}{4 [M(\epsilon_+, \frac{1}{2}, \sigma) U(\epsilon_-, \frac{1}{2}, \sigma) \lambda^2 + M(\epsilon_1, \frac{1}{2}, \sigma) U(\epsilon_+, \frac{1}{2}, \sigma) \nu]} \right\}. \quad (13)$$

For the better transparency, we use the following notations  $\epsilon_- = \frac{2\lambda^2 - \nu}{\nu}$ ,  $\epsilon_+ = \frac{2\lambda^2 + \nu}{\nu}$  and  $\sigma = \frac{(4\lambda - \omega)^2}{4\nu}$ . Figure 10 presents the shape function for the blue noise. It shows some similar features to the former white noise. The solution on the positive axis can be interpreted only on two separate finite intervals. The function has finite values, however, the first derivatives at the right hand side of the intervals become infinite, which can be interpreted as a kind of "semi-cusp". With some vertical shifts parallel to the axis  $f(\omega)$  the solution can be physically interpreted as two distinct islands growing in time. As an additional fineness, we note that at left side of the right island there is a gap.

Figure 11 shows the solution function  $u(x, t)$  of the original PDE. The spatial range of the two distinct intervals is continuously growing in time, however, it remains separate even at infinite times. With this kind of noise and Ansatz, there is no way to grow a constant surface above the whole positive semi-axis.

#### 4.5 Gaussian noise

The first non-power law noise gives us the ODE of

$$\nu f''(\omega) + f'(\omega) \left[ \frac{\omega}{2} + \frac{\lambda}{2} f'(\omega) \right] + a e^{-\frac{\omega^2}{n}} = 0. \quad (14)$$

There is no general formula available for arbitrary parameters  $\lambda, \eta, a$  and  $n$ . Fortunately, if two parameters are fixed e.g.  $\nu = 1/2$  and  $n = 1$ , then there is a closed expression available for the solution

$$f(\omega) = -\frac{1}{2\lambda} \ln \left[ 1 + \tan \left\{ \sqrt{\lambda a \pi} \cdot \operatorname{erf} \left( \sqrt{\frac{\omega}{2}} \right) + c_1 \right\}^2 \right] + c_2, \quad (15)$$

where  $\operatorname{erf}$  means the error function [30]. Figure 12 presents various solutions for different values of  $\lambda$ . The larger the value  $\lambda$  and the smaller the parameter  $a$  the more the number of initial islands are, which is a remarkable new feature. The solution itself is a continuous function on the whole  $\omega$  axis. The Van Hove singularities at finite  $\omega$  are still present. Note, that at larger value of  $\lambda$ , the depth of the singularity valleys become shallower.

Figure 13. presents the final solution of the PDE. The general features are very similar to the formerly investigated noise  $a/\omega^2$  but now three independent islands increases as time goes on. The islands never grow together, the valleys stay present even at large time.

At this point we mention, that for the exponential distribution  $\eta = e^{-\omega/a}$  as noise term, there is no analytic solution available at all.

#### 4.6 Lorentzian noise

As last system we have to investigate the ODE of

$$\nu f''(\omega) + f'(\omega) \left[ \frac{\omega}{2} + \frac{\lambda}{2} f'(\omega) \right] + \frac{a}{1 + \omega^2} = 0. \quad (16)$$

Unfortunately, the general solution cannot again be given in a closed form. In the formal solution some integrals of the Heun functions remain. For positive and given parameters  $\nu, \lambda$ , the solution becomes well-defined. As an example for  $a = 1/2, \lambda = 2$  and  $\nu = 1/2$ , the shape function reads

$$\begin{aligned} f(\omega) = & -\frac{\omega^2}{4} + \frac{\ln(2)}{2} + \frac{1}{2} \ln \left\{ \left[ -c_2 \omega H_C \left( -\frac{1}{2}, \frac{1}{2}, 1, \frac{1}{8}, \frac{7}{8}, -\omega^2 \right) + \right. \right. \\ & \left. \left. c_1 H_C \left( -\frac{1}{2}, -\frac{1}{2}, 1, \frac{1}{8}, \frac{7}{8}, -\omega^2 \right) \right] / \right. \\ & \left[ -2\omega^4 H_C \left( -\frac{1}{2}, -\frac{1}{2}, 1, \frac{1}{8}, \frac{7}{8}, -\omega^2 \right) H_{CPrime} \left( -\frac{1}{2}, \frac{1}{2}, 1, \frac{1}{8}, \frac{7}{8}, -\omega^2 \right) + \right. \\ & 2\omega^4 H_{CPrime} \left( -\frac{1}{2}, -\frac{1}{2}, 1, \frac{1}{8}, \frac{7}{8}, -\omega^2 \right) H_C \left( -\frac{1}{2}, \frac{1}{2}, 1, \frac{1}{8}, \frac{7}{8}, -\omega^2 \right) + \\ & \omega^2 H_C \left( -\frac{1}{2}, -\frac{1}{2}, 1, \frac{1}{8}, \frac{7}{8}, -\omega^2 \right) H_C \left( -\frac{1}{2}, \frac{1}{2}, 1, \frac{1}{8}, \frac{7}{8}, -\omega^2 \right) + \\ & 2\omega^2 H_{CPrime} \left( -\frac{1}{2}, -\frac{1}{2}, 1, \frac{1}{8}, \frac{7}{8}, -\omega^2 \right) H_C \left( -\frac{1}{2}, \frac{1}{2}, 1, \frac{1}{8}, \frac{7}{8}, -\omega^2 \right) - \\ & 2\omega^2 H_C \left( -\frac{1}{2}, -\frac{1}{2}, 1, \frac{1}{8}, \frac{7}{8}, -\omega^2 \right) H_{CPrime} \left( -\frac{1}{2}, \frac{1}{2}, 1, \frac{1}{8}, \frac{7}{8}, -\omega^2 \right) + \\ & \left. \left. H_C \left( -\frac{1}{2}, -\frac{1}{2}, 1, \frac{1}{8}, \frac{7}{8}, -\omega^2 \right) H_C \left( -\frac{1}{2}, \frac{1}{2}, 1, \frac{1}{8}, \frac{7}{8}, -\omega^2 \right) \right] \right\} \end{aligned} \quad (17)$$

where  $H_C$  and  $H_{CPrime}$  means the Heun functions and the derivative of the Heun  $C$  function, respectively [30]. Figure 14 shows the shape function for the Lorentzian noise term. The new feature compared to the former Gaussian noise term is that the domain of the solution is just a finite interval. Just a single island is born at the beginning of the surface growth process. The solution blows up (or blows down) on a finite one is the compact support of the solution. The last figure (Fig. 15) presents the final solution of the KPZ PDE. The solution has a compact support as well. It means that the small island which was positioned at the origin just grows for large times, but cannot diffuse onto the whole surface.

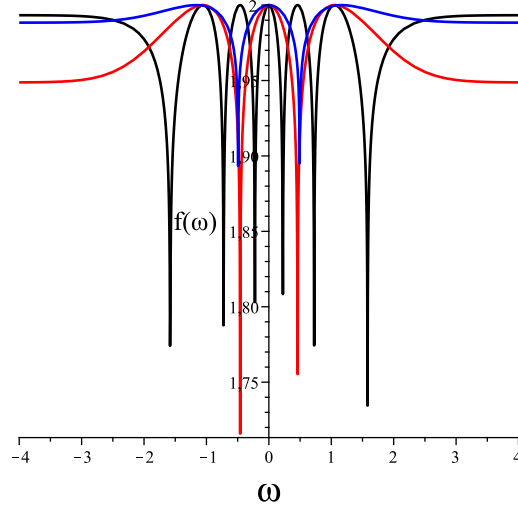


Figure 12: Various shape functions of Eq.(15) for the parameter set  $\nu = 1/2$ ,  $n = 1$ ,  $c_2 = 1$  and  $c_1 = 0$  for different  $\lambda$  values. Black, red and blue lines are for  $a = 1$ ,  $\lambda = 25$ ,  $a = 0.25$ ,  $\lambda = 25$ , and  $a = 0.1$ ,  $\lambda = 55$ , respectively.

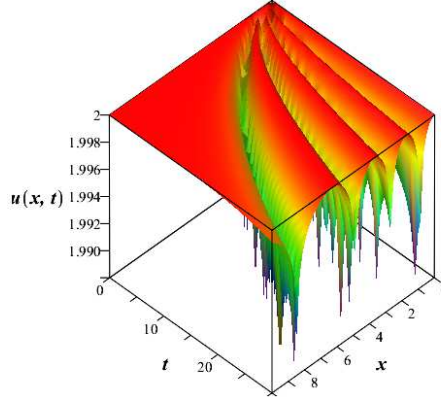


Figure 13: The complete solution for the Gaussian noise for  $a = 0.1$ ,  $\lambda = 55$  value. Other parameters are unchanged.

## Conclusions

In summary we can say that with an appropriate change of variables applying the self-similar Ansatz one may obtain analytic solution for the KPZ equation for one spatial dimension with numerous noise terms. We investigated four power-law-type noise  $\omega^n$  with exponents of  $-2, -1, 0, 1$ , called the brown, pink, white and blue noise, respectively. Each integer exponent describes completely different dynamics. Additionally, we investigated the properties of Gaussian and Lorenzian noises. Providing completely dissimilar surfaces with growth dynamics. All solutions can be described with non-trivial combinations of various special functions, like error, Whittaker, Kummer or Heun. The parameter dependencies of the solutions are investigated and discussed. Future works are planned for the investigations of the two dimensional surfaces.

We also remark that applying transformations  $k = e^{\frac{\lambda}{2\nu}u}$ ,  $k = t^\alpha m(z)$  and  $z = xt^{-\beta}$  to equation (1), one gets the linear ordinary differential equation  $m'' + \frac{1}{2}zm' + (\frac{\lambda}{2\nu}t\eta - \alpha)m = 0$  for any arbitrary value of  $\alpha$  and  $\beta = 1/2$ .

## Acknowledgment

This work was supported by Project no. 129257 implemented with the support provided from the National Research, Development and Innovation Fund of Hungary, financed under the  $K_{18}$  funding scheme.

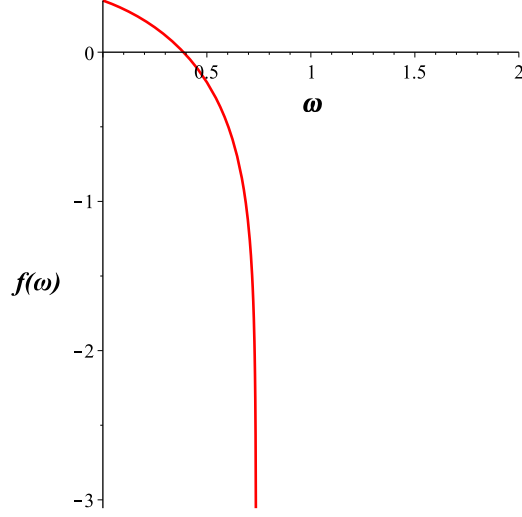


Figure 14: The shape function for the Lorenz noise for  $a = 1/2$ ,  $\lambda = 2$ ,  $\nu = 1/2$  and for  $c_1 = c_2 = 1$ .

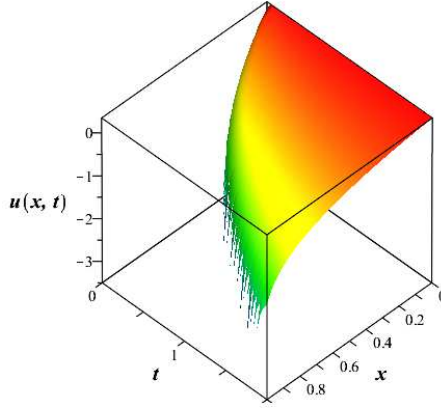


Figure 15: The complete solution  $u(x, t)$  for the Lorenz noise with the parameters given above.

## References

- [1] A. Pimpinelli and J. Villain. *Physics of Crystal Growth*. Cambridge University Press, 1998.
- [2] G. Parisi M. Kardar and Yi-C. Zhang. Dynamic scaling of growing interfaces. *Phys. Rev. Lett.*, 56:889, 1986.
- [3] A.-L. Barabási and H. E. Stanley. *Fractal concepts in surface growth*. Press Syndicate of the University of Cambridge, 1995.
- [4] T. Hwa and E. Frey. Exact scaling function of interface growth dynamics. *Physical Review A*, 44(12):R7873, 1991.
- [5] E. Frey, U. C. Täuber, and T. Hwa. Mode-coupling and renormalization group results for the noisy burgers equation. *Physical Review E*, 53(5):4424, 1996.
- [6] M. Lässig. On growth, disorder, and field theory. *Journal of physics: Condensed matter*, 10(44):9905, 1998.
- [7] T. Kriecherbauer and J. Krug. A pedestrian’s view on interacting particle systems, kpz universality and random matrices. *Journal of Physics A: Mathematical and Theoretical*, 43(40):403001, 2010.
- [8] M. Einax, W. Dieterich, and P. Maass. Colloquium: Cluster growth on surfaces: Densities, size distributions, and morphologies. *Reviews of modern physics*, 85(3):921, 2013.
- [9] M. Matsushita, J. Wakita, H. Itoh, I. Rafols, T. Matsuyama, H. Sakaguchi, and M. Mimura. Interface growth and pattern formation in bacterial colonies. *Physica A: Statistical Mechanics and its Applications*, 249(1-4):517–524, 1998.

- [10] Y. Kuramoto and T. Tsuzuki. Persistent propagation of concentration waves in dissipative media far from thermal equilibrium. *Progress of theoretical physics*, 55(2):356–369, 1976.
- [11] G. I. Sivashinsky. Large cells in nonlinear marangoni convection. *Physica D: Nonlinear Phenomena*, 4(2):227–235, 1982.
- [12] M. Guedda and R. Kersner. Self-similar solutions to the generalized deterministic kpz equation. *Nonlinear Differential Equations and Applications NoDEA*, 10(1):1–13, 2003.
- [13] R. Kersner and M. Vicsek. Travelling waves and dynamic scaling in a singular interface equation: analytic results. *Journal of Physics A: Mathematical and General*, 30(7):2457–2465, 1997.
- [14] J. Kelling, G. Ódor, and S. Gemming. Suppressing correlations in massively parallel simulations of lattice models. *Computer Physics Communications*, 220:205–211, 2017.
- [15] T. Martynec and S. H. L. Klapp. Impact of anisotropic interactions on nonequilibrium cluster growth at surfaces. *Phys. Rev. E*, 98:042801, Oct 2018.
- [16] D. Sergi, A. Camarano, J. M. Molina, A. Ortona, and J. Narciso. Surface growth for molten silicon infiltration into carbon millimeter-sized channels: Lattice–boltzmann simulations, experiments and models. *International Journal of Modern Physics C*, 27(06):1650062, 2016.
- [17] B. A. Mello. A random rule model of surface growth. *Physica A: Statistical Mechanics and its Applications*, 419:762–767, 2015.
- [18] P. Calabrese, P. L. Doussal, and A. Rosso. Free-energy distribution of the directed polymer at high temperature. *EPL (Europhysics Letters)*, 90(2):20002, 2010.
- [19] T. Sasamoto and H. Spohn. One-dimensional kardar-parisi-zhang equation: an exact solution and its universality. *Physical review letters*, 104(23):230602, 2010.
- [20] P. Calabrese and P. L. Doussal. Exact solution for the kardar-parisi-zhang equation with flat initial conditions. *Physical review letters*, 106(25):250603, 2011.
- [21] P. L. Doussal and T. Thiery. Diffusion in time-dependent random media and the kardar-parisi-zhang equation. *Physical Review E*, 96(1):010102, 2017.
- [22] L. Mátyás and P. Gaspard. Entropy production in diffusion-reaction systems: The reactive random lorentz gas. *Physical Review E*, 71(3):036147, 2005.
- [23] L. Mátyás, T. Tél, and J. Vollmer. Multibaker map for shear flow and viscous heating.
- [24] I. F. Barna, G. Bognár, and K. Hriczó. Self-similar analytic solution of the two-dimensional navier-stokes equation with a non-newtonian type of viscosity. *Mathematical Modelling and Analysis*, 21(1):83–94, 2016.
- [25] I. F. Barna and R. Kersner. Heat conduction: a telegraph-type model with self-similar behavior of solutions. *Journal of Physics A: Mathematical and Theoretical*, 43(37):375210, 2010.
- [26] L. I. Sedov. *Similarity and dimensional methods in mechanics*. CRC press, 1993.
- [27] I. F. Barna and L. Mátyás. Analytic solutions for the one-dimensional compressible euler equation with heat conduction and with different kind of equations of state. *Miskolc Mathematical Notes*, 14(3):785–799, 2013.
- [28] I. F. Barna. Self-similar solutions of three-dimensional navier—stokes equation. *Communications in Theoretical Physics*, 56(4):745, 2011.
- [29] I. F. Barna. Self-similar analysis of various navier-stokes equations in two or three dimensions. In D. Campos, editor, *Handbook on Navier-Stokes Equations*, Theory and Applied Analysis, New York, 2017. Nova Publishers.
- [30] W. J. F. Olver, D. W. Lozier, R. F. Boisvert, and C. W. Clark. *NIST handbook of mathematical functions hardback and CD-ROM*. Cambridge University Press, 2010.
- [31] L. Van Hove. The occurrence of singularities in the elastic frequency distribution of a crystal. *Physical Review*, 89(6):1189, 1953.
- [32] Z. Csahók, K. Honda, E. Somfai, M. Vicsek, and T. Vicsek. Dynamics of surface roughening in disordered media. *Physica A: Statistical Mechanics and its Applications*, 200(1-4):136–154, 1993.